



Signatures of aerosol-cloud interactions in GiOcean: A coupled global reanalysis with two-moment cloud microphysics

Ci Song¹, Daniel McCoy¹, Andrea Molod², and Donifan Barahona²

¹Department of Atmospheric Science, University of Wyoming

²Global Modeling and Assimilation Office, NASA Goddard Space Flight Center

Correspondence: Ci Song (csong@uwoyo.edu)

Abstract. Aerosols in the atmosphere affect top of atmosphere radiation through direct interactions with radiation and by affecting cloud properties. Through aerosol-cloud interactions (ACI), and ensuing adjustments, anthropogenic aerosols have led to cooling during the industrial era. However, there is substantial uncertainty in our global models regarding the cooling driven by ACI. In part, global models are subject to substantial disagreement in terms of cloud properties, thermodynamic state, hydrological cycle, and general circulation. Reanalysis provides a useful avenue for exploring the impact of ACI on clouds and radiation because its atmosphere is nudged to observations of these quantities, but until now reanalyses have not included two-moment microphysics coupled to aerosols. Here, we explore the impact of ACI on clouds in the GiOcean reanalysis—the first to incorporate aerosol-cloud adjustments. We develop source-sink models of ACI in GiOcean and contrast these to satellite observations and allow attribution of changes in cloud droplet number (Nd) and liquid water path (LWP) to aerosol and meteorology.

1 Introduction

The change in reflected solar radiation due to anthropogenic emissions of aerosols (e.g., aerosol forcing) is largely uncertain due to the complex effects that aerosols can have on climate (Bellouin et al., 2019). Aerosols affect the top of atmosphere radiation by different ways. Aerosol alters the Earth's energy budget directly by scattering and absorption of radiation, termed as aerosol radiation interaction. Aerosol can affect climate indirectly by aerosol-cloud interactions (ACI) by 1) modifying cloud microphysical properties, and altering their reflectivity, termed as Twomey effect (Twomey, 1977), and 2) by altering macrophysical properties induced by changes in cloud microphysics (Ackerman et al., 2004), such as cloud lifetime, precipitation formation and cloud cover, denoted as aerosol-cloud adjustment (Albrecht, 1989; Bretherton et al., 2007). ACI and ensuing adjustment have led to cooling during the industrial era, termed as aerosol indirect forcing., but the degree to which ACI have affected the Earth's energy budget remains the largest uncertainty (Bellouin et al., 2019).

We can infer climate sensitivity from the observed temperature record and the historical radiative forcing. Due to the uncertainty in climate sensitivity engendered by ACI, numerous researchers have attempted to study ACI using observations and modeling techniques. Observations of aerosol, clouds, precipitation and radiation flux at the top of atmosphere (TOA) necessary to study ACI, are available from various of surface sites, airborne and remote sensing measurements. Modeling at a variety



25 of scales is needed as it bridges the gap between Global Climate Models (GCMs) and observations through intermediate scales
from convection-permitting and eddy-resolving simulations. However, both observations and modeling suffer from uncertain-
ties. In-situ observations are sparse in sampling within a complex and chaotic system (Field and Furtado, 2016). Spaceborne
remote sensing can retrieve both aerosol and cloud properties with nearly global coverage, but they must do this indirectly
using remote sensing whose retrievals are typically based on averaged conditions for which the algorithms used for deriving
30 aerosol and cloud properties are not always valid (Grosvenor and Wood, 2014a). On the other hand, GCMs do not have prob-
lems in sampling in terms of time and space but their representation of cloud, aerosol, precipitation, and other processes that
are important to ACI is parameterized and may be missing key processes altogether (Regayre et al., 2023).

Cloud microphysical processes are hard to represent in GCMs as these processes are small in scale ($\sim \mu\text{m}$) and GCMs (1°)
cannot resolve these small, fast processes. Parameterization of cloud microphysics is needed in GCMs for the foreseeable fu-
35 ture. Representing billions of individual raindrop or ice crystal clouds in GCMs is difficult due to the excessive computational
expenses. Therefore, cloud microphysics parameterizations in GCMs are simplified to 'bulk' schemes, assuming a fixed math-
ematical form for the particle size distributions. Bulk microphysics schemes use one or more "moments" of the particle size
distribution (PSD) to describe the hydrometeors. A one-moment scheme usually predicts only the mass concentration of cloud
droplets and ice crystals with unchanged-prescribed distribution of number concentration or effective radius of cloud particles
40 (e.g., droplets and crystals). However, the evolution of droplet number concentration and droplet size distribution with aerosol
perturbations is not captured by one-moment microphysics scheme. In reality, increase in aerosol particles typically leads to
more but smaller cloud droplets, given the same amount of cloud water and the increasing number of smaller droplets reflect
more solar radiation back to space due to increased scattering cross section, leading to a cooling effect on the Earth's surface
(Twomey, 1977). Therefore, the lack of representation of droplet number concentration and effective radius in one-moment
45 schemes results in the less robust interaction between aerosols and clouds in models, and by extension the representation of
aerosol indirect forcing. Two-moment schemes predict both the mass and the number concentration of cloud droplets and ice
crystals using prognostic equations, and the evolution of the cloud particle size distribution is explicitly calculated, which pro-
vides a linkage between aerosol emissions and cloud properties by activation of cloud droplet and ice nucleation (Barahona
et al., 2014b). Therefore, the impact of atmospheric aerosols on clouds can be explicitly represented in GCMs. Many GCMs
50 have implemented the two-moment microphysics scheme into cloud presentations and showed improved representation of
cloud properties (Ghan et al., 1997; Lohmann et al., 1999; Ming et al., 2007; Barahona et al., 2014b; Morrison and Gettelman,
2008).

The radiative forcing from aerosol has a large spatial variability; regionally it can be either positive or negative (IPCC, 2013).
Several factors contribute to such a heterogeneity. Aerosol have a shorter lifespan in the atmosphere than greenhouse gases, of
55 the order of few days to about two weeks. Despite this, they may be transported around the globe and interact with clouds and
radiation far away from their sources (Uno et al., 2009). Over this time their composition may change due to the interaction
with local pollution sources and from oxidation processes. When aerosol particles reach pristine regions in the North Atlantic
and the Pacific oceans, away from their emission sources, they may substantially impact the regional climate (Fan et al., 2016).
Their emission rate changes over time, with marked seasonal cycles (McCoy et al., 2017; Kasibhatla et al., 1997), and long-



60 term decadal trends (Bellucci et al., 2015; McCoy et al., 2018a). Volcanic events and even policy decisions (Yuan et al., 2024) add variability to the atmospheric aerosol concentration (Bellucci et al., 2015). It is known that over the time scale of days to months, aerosols have an observable, local effect on clouds and radiation (Fan et al., 2016; Breen et al., 2020). These effects can result in persistent radiative flux and cloud property anomalies, strong enough to modify large scale atmospheric patterns (Morcrette et al., 2011; Bellucci et al., 2015; Ekman, 2012).

65 The interaction of aerosol with climate is typically neglected in operational forecasting systems and climate reanalyses. In reanalyses that include an aerosol representation, a carefully crafted aerosol climatology is allowed to interact with radiation as a way of representing the aerosol direct effect, however neglecting ACI (e.g., Bozzo et al., 2020). This approach has shown to improve the prediction of the African Easterly Jet (Tompkins et al., 2005) and tropical cyclogenesis (Reale et al., 2014). On the other hand, Zhang et al. (2016a) showed that numerical weather prediction (NWP) systems using aerosol climatologies
70 overestimated surface temperature during a strong biomass burning event, whereas models with prognostic aerosols showed the correct surface cooling. In some cases the usage of aerosol climatologies may lead to degradation of the forecast skill, since without the feedback between aerosol and meteorology, anomaly centers associated with aerosol emissions become permanent, imprinting spurious temperature gradients that perturb global circulation (Morcrette et al., 2011). Ekman (2014) suggested that the explicit representation of ACI in climate models improves the simulation of the historical surface temperature trend. This
75 has been further shown during dust storms over Europe and north Africa where neglecting dust emissions and their effect on clouds can lead to overestimation of surface temperature in NWP (Bangert et al., 2012). Aerosol effects have been shown to play a significant role in the modulation of dust transport by the Madden Julian Oscillation (MJO) (Benedetti and Vitart, 2018) as well on hurricane development (Nowotnick et al., 2018). Given all of these potential interactions between aerosol and climate, there is a growing consensus that ACI must be represented in weather, seasonal forecasting models, and climate
80 reanalyses (Board et al., 2016).

This study introduces a new coupled reanalysis dataset - GiOcean, which incorporates two-moment microphysics scheme for stratiform and convective clouds, enabling the explicit representation of ACI (Barahona et al., 2014b; Molod et al., 2020b). We focus on evaluating the impact of ACI in warm clouds by comparing it with observations of clouds, precipitation, and aerosol during periods of substantial emission changes over a multidecadal time scale. Cloud droplet number concentration
85 (Nd) and liquid water path (LWP) are two important microphysical and macrophysical cloud properties in evaluating ACI (Bellouin et al., 2019). Look up tables of Nd and LWP as a function of their sinks and sources are built up for both GiOcean reanalysis data and remote sensing observations, respectively. Sensitivity tests are applied for the look up tables of Nd and LWP by forcing their sources and sinks a constant, respectively. While the large scale meteorological aspects of GiOcean will be analyzed in future studies, we show that GiOcean allows for the assessment of the sensitivity of key ACI variables (e.g., Nd
90 and LWP) to their sinks and sources relative to remote sensing observations.



2 Methods

2.1 The GiOcean Coupled Reanalysis

GiOcean is a "one-way coupled" reanalysis that spans from 1998 to the present, with a time lag of approximately six months. It includes atmosphere, aerosol, ocean, and sea ice components with spatial resolutions of approximately 50 km for the atmosphere and 25 km for the ocean. Data assimilation is based on the Global Earth System Model Subseasonal-to-Seasonal (GEOS-S2S) prediction system (Molod et al., 2020b). The main components of the GEOS-S2S are the GEOS Atmospheric Global Circulation Model (AGCM) (Molod et al., 2015; Rienecker et al., 2008), the catchment land surface model (Koster et al., 2000), the MOM5 ocean general circulation model (Griffies et al., 2005; Griffies, 2012), and the Community Ice CodE-4 sea ice model (Hunke, 2008). Ocean data assimilation follows the Local Ensemble Transform Kalman Filter approach (Penny et al., 2013). All components are coupled together using the Earth System Modeling Framework (Hill et al., 2004) and the Modeling Analysis and Prediction Layer interface layer (Suarez et al., 2007). GEOS-IT, produced for NASA's instrument teams, serves as a stable meteorological dataset for GiOcean (https://gmao.gsfc.nasa.gov/GMAO_products/GEOS-5_FP-IT_details.php). Similar to the Modern-Era Retrospective Analysis for Research and Applications, Version 2 (MERRA-2) (Gelaro et al., 2017b), GEOS-IT is a multidecadal retrospective reanalysis integrating both aerosol and meteorological observations (Gelaro et al., 2017b; Randles et al., 2017). However, it incorporates recent model enhancements that provide more accurate representations of moisture, temperature, and land surfaces as well as the latest satellite observations through updated analysis techniques.

The NASA GEOS system serves as the modeling foundation for GiOcean. In GEOS-AGCM, transport of aerosols and gaseous tracers such as CO are simulated using the Goddard Chemistry Aerosol and Radiation model (GOCART; Colarco et al., 2010). Aerosols being both interactive and radiatively active, thus allowing GiOcean to represent the aerosol direct effect. GOCART is a mass-based aerosol transport model that explicitly calculates the transport and evolution of dust, black carbon, organic material, sea salt, and sulfate. Prescribed size distributions were used to calculate mass-number conversion factors as detailed by Barahona et al. (2014a). Dust and sea salt emissions are prognostic whereas sulfate and biomass burning data are prescribed (Randles et al., 2017). Volcanic SO₂ emissions are constrained by observations from the Ozone Monitoring Instrument (OMI) on-board NASA's EOS/Aura spacecraft (Carn et al., 2017a). Aerosol fields are assimilated using The Goddard Aerosol Assimilation System (Buchard et al., 2016b), with the overall cycle controlled by meteorology.

Aerosol assimilation uses the Goddard Aerosol Assimilation System (GAAS), and is carried out in two steps. First the aerosol optical depth (AOD), is assimilated using the observing system described in Table 2 of Randles et al. (2017). Then in a second step the analysis increment is distributed vertically and among the different aerosol species to update their mass mixing ratios. In GiOcean the overall assimilation cycle is controlled by the meteorology. The meteorological observing system is also much larger than the one used in GAAS (Gelaro et al., 2017b). Thus GAAS can be seamlessly and efficiently run using a previously generated meteorological analysis. This feature was used by Buchard et al. (2016a) to generate the version 1 of the Modern Era Retrospective analysis for Research and Applications aerosol reanalysis (MERRAero), by "replaying" (Takacs et al., 2018) the MERRA-1 meteorological fields, and by direct assimilation of AOD in MERRA-2. However in both cases



clouds were driven by a single moment cloud microphysical scheme and neither MERRA-2 nor MERRAero had a direct link
125 between aerosol and clouds hence lacked a representation of the aerosol indirect effect.

Of significance to this work is that cloud microphysics is described using a two-moment scheme, allowing GiOcean to
explicitly represent the aerosol indirect effect. The microphysics scheme calculates the mixing ratio and number concentration
of cloud droplets and ice crystals as prognostic variables for stratiform clouds, and convective clouds (i.e., stratocumulus,
cirrus) (Barahona et al., 2014a). Cloud droplet activation is parameterized using the approach of Abdul-Razzak and Ghan
130 (2000). Ice crystal nucleation is estimated using a physically-based analytical approach (Barahona and Nenes, 2009) that
includes homogeneous and heterogeneous ice nucleation, and their competition. The description of heterogeneous ice droplet
formation by immersion freezing and contact ice nucleation follows (Ullrich et al., 2017; Tan and Barahona, 2022). Vertical
velocity fluctuations are constrained by non-hydrostatic, high-resolution global simulations (Barahona et al., 2017). Using this
configuration GEOS has been shown to reproduce the global distribution of clouds, radiation, and precipitation in agreement
135 with satellite retrievals and *in situ* observations (Barahona et al., 2014a; Molod et al., 2020b).

2.2 Observations

2.2.1 MODIS Nd and AOD

Throughout this study, the aerosol metric we used was the AOD, which is the column-integrated aerosol amount. Although
AOD does not provide information for the vertical distribution of aerosols or the aerosol sizes and species in the column,
140 remotely-sensed AOD provides an estimate of column integrated aerosol loading nearly globally, in contrast to sparse in-situ
observations of aerosols made by aircraft, and can be compared relatively directly between models and observations. In this
work, observations of AOD for the period of 2003–2015 are taken from a passive imaging radiometer - Moderate Resolution
Imaging Spectroradiometer Collection 6 (MODIS C6), retrieved at 550 nm on the Aqua (1:30 P.M. local solar Equatorial
crossing time) platform.

Nd is key in understanding processes associated with ACI (Wood, 2012). Knowledge of the spatial and temporal variability of
Nd is of importance for gaining insights into ACI. Observations of Nd in this study are derived from cloud optical thickness (τ_c)
and cloud effective radius (r_e) retrievals from MODIS C6 for the period of 2003–2015 based on adiabatic clouds assumptions
(Grosvenor et al., 2018). τ_c and r_e are simultaneously retrieved by a bispectral algorithm that relies on the cloud reflectance
measured from both a non-absorbing visible wavelength and an absorbing shortwave infrared wavelength (Nakajima and
150 King, 1990; Zhang et al., 2016b). MODIS Nd has been shown to be un-biased relative to in-situ measurements from aircraft
and provides nearly global coverage of observations (Gryspeerdt et al., 2022). However, there are several potential sources
of uncertainty that affect the Nd calculated from this method including low sun-angle (Grosvenor and Wood, 2014b), cloud
heterogeneity (Grosvenor et al., 2018), and contamination by upper level cloud and aerosol (Zhang et al., 2016b).



2.2.2 MAC-LWP

155 Cloud liquid condensate mass provides a diagnostic of the liquid cloud adjustment to aerosol-induced changes in cloud micro-
physics (Bellouin et al., 2019; Song et al., 2024). In practice, liquid condensate mass is usually observed as column-integrated
liquid water from remote sensing observations, which is known as liquid water path (LWP). In this study, we took observations
of LWP from the Multi-Sensor Advanced Climatology of Liquid Water Path (MAC-LWP) for the period 2003–2015 (Elsaesser
et al., 2017). MAC-LWP is an updated version of the University of Wisconsin (UWisc) cloud LWP (CLWP) climatology
160 (O'Dell et al., 2008). Oceanic monthly-mean MAC-LWP at 1 ° spatial resolution is constructed from 7 sources of satellite
microwave data sampling different parts of the diurnal cycle at 0.25° spatial resolution. One of the major updates to UWisc
LWP is that the MAC-LWP bias was corrected by matchups to clear-sky scenes from MODIS in cases where clear-sky is
observed but non-zero cloud LWP is retrieved due to retrieval cross-talk. Because it is difficult to differentiate cloudwater from
rainwater using passive microwave signal from cloudwater, uncertainty in MAC-LWP is usually larger in heavy-precipitating
165 regions (Elsaesser et al., 2017).

2.2.3 IMERG

Observations of precipitation are taken from the Integrated Multi-satellitE Retrievals for Global Precipitation Mission (IMERG)
(Huffman et al., 2020). IMERG is a merged precipitation product that contains information from passive microwave precipita-
tion estimates, microwave-calibrated infrared (IR) satellite estimates, gauge analyses, and other estimators via intercalibrating,
170 merging, and interpolating the sources of precipitation estimates. IMERG provides precipitation data with global coverage
spanning the entire Tropical Rainfall Measuring Mission (TRMM) and the Global Precipitation Measurement (GPM) mission
record. In this study, we used IMERG version 07 (V07) final run daily data for the period of 2003-2015 for analysis (Huffman
et al., 2023).

3 Results

175 3.1 Spatial variability

This study focuses on the evaluation of ACI in warm clouds in GiOcean. We limit the scope of our study to examining variables
related to the amount of aerosol, its activation into droplets, and the changes in the cloud macrophysical state and precipitation
rate in response to changes in cloud microphysics (aerosol-cloud adjustments). We focus on variables that can be compared
relatively directly between GiOcean and spaceborne remote sensing: AOD, Nd, LWP and precipitation rate.

180 AOD provides a column integrated estimate of aerosol. AOD is not a direct analogy for the amount of aerosol that is
relevant to the budget of cloud condensation nuclei available to liquid clouds because it does not directly characterize size
distribution and chemistry and is column integrated. However, it does provide a measure of the column loading of aerosol
that can be compared relatively directly between GiOcean and observations from spaceborne remote sensing. AOD from
GiOcean compares favorably to MODIS AOD with similar AOD in regions of heavy anthropogenic pollution, Saharan dust,



185 and biomass burning (Figure 1ab). MODIS AOD at high latitudes is noticeably affected by lack of clear skies and surface contamination, particularly in the northern hemisphere. This is particularly striking in the zonal-mean (Figure 2a). AOD in GiOcean is systematically low in the Southern Ocean compared to MODIS (Figure 2a). GiOcean AOD is assimilated from AOD measurements collected by both the Terra and Aqua satellites (Buchard et al., 2016b). The Terra satellite crosses the equator in the morning, while the Aqua satellite crosses in the afternoon. Since AOD is influenced by the diurnal cycle (Balmes et al., 190 2021), this difference in crossing times should result in differences in the AOD observed between the two satellites. Contrasting satellite AOD sampled during a given overpass should also lead to small discrepancies relative to the GiOcean AOD that is averaged over the day (Figure 2a). Several drivers may enhance this disagreement since they may cause divergence between the assimilated and observed AOD including: the effects of aerosol humidification (Twohy et al., 2009) and lack of cloudiness in GiOcean in this region, lack of new particle formation events (McCoy et al., 2021; Gordon et al., 2017), or simply a lack of aerosol in the pristine Southern Ocean. Lower AOD in GiOcean is also apparent in the area downwind from Kīlauea and Vanuatu, which are areas of substantial effusive volcanic emissions (McCoy et al., 2018a; Carn et al., 2017b) (Figure 1ab). Volcanic SO₂ emissions in GiOcean are constrained by observations from the Ozone Monitoring Instrument (OMI) on board NASA's EOS/Aura spacecraft (Carn et al., 2015). The dataset however only provides annual SO₂ emission rates. Such an approach however fails to capture degassing events, as for example for Kilauea in 2008 and 2018, for which daily varying 195 emissions are required (Breen et al., 2021).

There are qualitative similarities between GiOcean Nd and MODIS Nd over oceans (Figure 1cd). Nd is high in the anthropogenically perturbed regions near heavily-industrialized regions and in the outflow of biomass burning in Namibia and Saharan dust, consistent with regions of enhanced AOD (Figure 1ab). A significant difference in Nd between GiOcean and MODIS is that GiOcean has a much larger range of Nd with high Nd near aerosol sources and low Nd in pristine, remote ocean 205 regions compared to MODIS. In Figure 1 we highlight the outflow regions from North America and East Asia. These regions have been characterized in previous studies examining Nd variability (McCoy et al., 2018a) and have relatively high Nd in both GiOcean and MODIS. We will focus on these regions through the remainder of our study. Overall, the dominance of relatively pristine regions in the oceanic zonal-mean is apparent with lower zonal-mean Nd over oceans in GiOcean than observed by MODIS (Figure 2). This is especially pronounced in the remote Southern Ocean, which is a long-standing problem for global 210 models and relevant to our understanding of aerosol forcing (McCoy et al., 2020b; Mulcahy et al., 2018).

Liquid water path is systematically lower in GiOcean than observed by microwave radiometers as aggregated and harmonized in the MAC-LWP data set (Figure 1ef and Figure 2c). However, some of this discrepancy may be attributable to potential systematic errors in microwave LWP as discussed in section 2.2.2. Within the extratropics we estimate this error to be $\pm 10\%$ (Song et al., 2024; Elsaesser et al., 2017), which may bring the observations closer, but cannot entirely explain this observation- 215 reanalysis discrepancy (Figure 2c). The discrepancy is larger in relatively low precipitation regions in the subtropics. Overall this points to a lower LWP in GiOcean, despite observational uncertainty.

Precipitation rate in GiOcean is consistent with IMERG observations in both the zonal-mean (Figure 2d) and in spatial variability (Figure 1gh). Some slight disagreement is apparent in a sharper transition to very low rain rates in the subtropical dry zones near the western side of continents in GiOcean (Figure 1gh). This may be partially attributable to biases in GiOcean, but



220 may also relate to IMERG struggling to detect the prevalent drizzle in this region (Pradhan and Markonis, 2023). Precipitation rate in heavy-precipitating tropics is relatively lower in GiOcean .

The variable of state linking aerosol and clouds is the Nd (Wood, 2012). While the patterns of Nd in GiOcean and MODIS are qualitatively similar, there is a broad discrepancy between the datasets in the polluted to pristine gradient away from continents (Figure 1cd). Cloud droplet number is an approximate steady-state balance between CCN activating into cloud
225 droplets and removal of cloud droplets through evaporation or precipitation (Wood et al., 2012). While there is no global observation of CCN, we can examine AOD as a proxy for this term (Figure 1ab). AOD from GiOcean and MODIS are in good agreement except at very high latitudes (Figure 1ab). This is not entirely surprising since MODIS AOD is assimilated in GiOcean. AOD is not a direct proxy for liquid-cloud relevant CCN since it doesn't directly relate to size or contain information about hygroscopicity and is column integrated, but the agreement in AOD between GiOcean and MODIS supports relatively
230 similar sources of CCN. Similarly, precipitation rate from GiOcean is in good agreement with IMERG (Figure 2b). One caveat to this broad consistency is the stronger gradient in precipitation rate away from coasts over southern subtropics in GiOcean compared to IMERG (Figure 1gh), which could explain the relatively strong gradient of Nd away from the coast in GiOcean as a function of a too strong sink term of Nd as opposed to too strong a gradient in Nd sources.

A novel feature of the GiOcean reanalysis is that it has two-moment microphysics and the ability to produce precipitation
235 suppression and aerosol-cloud adjustments. Mean-state LWP contains information about aerosol-cloud adjustments in the context of the precipitation rate enforced by the environment through the large-scale circulation and the pattern of sea surface temperature (Song et al., 2024; Mikkelsen, 2024). The effects of the enforced convergence of moisture by the atmosphere and ocean are apparent in the similar precipitation rates in GiOcean and observations from IMERG (Figure 1gh). In this context, we can consider LWP as the amount of cloud needed to satisfy the precipitation flux enforced by the environment. While there
240 are many factors that can influence the precipitation efficiency in liquid cloud, Nd is important as it affects the precipitation efficiency by autoconversion in global models, where a increase in Nd results in precipitation suppression, and a increase in cloud amount satisfies stronger precipitation rate. (Khairoutdinov and Kogan, 2000; Michibata and Takemura, 2015; Jin and Nasiri, 2014). In this context, there is consistency between the lower Nd away from continental sources of aerosol in GiOcean relative to observations and the lower LWP in GiOcean given small differences in precipitation rate between GiOcean and
245 IMERG 1gh. The gradient of Nd from the coast into the ocean is steeper in GiOcean with lower Nd in GiOcean away from the coast (Figure 1cd). This is consistent with a higher precipitation rate in GiOcean and a lower amount of liquid cloud (Figure 1ef) needed to satisfy the precipitation rate demanded by the large-scale convergence of moisture.

Our characterization of aerosol amount, cloud droplet number, liquid cloudiness, and precipitation rate show regional biases in terms that act as sources of cloud droplet and cloud water as well as sinks in GiOcean. This highlights the need to examine
250 ACI in the context of steady state models of droplet number and liquid cloud mass. We will develop simple steady-state model characterizations of these terms in Section 3.3.



3.2 Seasonal cycle and decadal trends

Having characterized the spatial patterns in clouds, aerosol, and precipitation we examine temporal variability. We focus on the North American and East Asian outflow regions identified in Figure 1 and examine the seasonal and decadal variability in each region.

AOD seasonal variability agrees between GiOcean and MODIS (Figure 3ab). Peak AOD occurs in spring in the East Asian outflow region. In the North American outflow region it occurs in summer. While the AOD cycle agrees between GiOcean and MODIS with an explained variance of GiOcean by MODIS greater than 90%, seasonal cycles in Nd do not agree well and are negatively correlated. There is a pronounced seasonal cycle apparent in the East Asian region in GiOcean, but no seasonal cycle to speak of in MODIS (Figure 3c). GiOcean and MODIS generally agree that there is no seasonal cycle in the North American outflow region (Figure 3d).

The seasonal cycles of GiOcean and MAC-LWP are roughly in agreement with peak LWP occurring in winter in both regions (Figure 3ef). The better agreement between GiOcean and MAC-LWP during winter might be due to the relatively accurate MAC-LWP estimates during cold season over the study regions (Elsaesser et al., 2017). However, correlation between MAC-LWP and GiOcean is weakly negative in East Asia and the explained variance in GiOcean LWP by MAC-LWP is 60% in the North American outflow.

Seasonal variability in precipitation rate matches between GiOcean and IMERG (Figure 3gh). There is an explained variance in the East Asian outflow of near 100% where a strong seasonal cycle exists. In the North American outflow where the seasonal cycle is weaker there is only an explained variance 55%. High explained variance in GiOcean precipitation rate when there is a strong seasonal cycle is consistent with GiOcean assimilating towards sea surface temperature (SST) from GEOS-IT reanalysis data, as SST is a strong control of moisture convergence, and by extension precipitation, by the large-scale circulation (Seager et al., 2010).

The decadal trend in aerosol and cloud properties is a useful proxy for understanding the radiative forcing from ACI (Wall et al., 2022; McCoy et al., 2018a; Bennartz et al., 2011). Decadal trends in AOD, Nd, LWP, and precipitation rate in the focus regions match between GiOcean and observations (Figure 4).

Trends in AOD are in good agreement between GiOcean and MODIS (Figure 4ab). There is an overall downward trend in AOD in both focus regions in this study. This is consistent with trends in sulfur dioxide emissions in these regions driven by emissions control measures in the United States of America and Peoples Republic of China (McCoy et al., 2018a).

The trend in Nd from MODIS and GiOcean broadly agrees with the trend in AOD with a downward trend through the observational period (Figure 4cd). During the period with concurrent observational data (2003-2015) Nd shows an anti-correlation between GiOcean and MODIS and is relatively saturated in the East Asian outflow, while Nd decreases steadily in the North American outflow. This is consistent with previous evaluation of trends in Nd in these regions (McCoy et al., 2018a).

Decadal trends in LWP are relatively consistent between MAC and GiOcean (Figure 4ef). GiOcean has the microphysics necessary to produce precipitation suppression and this may lead to the qualitative agreement in the increase in LWP and Nd until around 2010 and then a decrease towards 2020 in the Asian outflow region in GiOcean. Decadal trend in LWP shows



relatively large interannual variability in the North American outflow and the LWP trend is broadly consistent with the trend in precipitation rate in GiOcean.

In keeping with the seasonal cycle, decadal trends in precipitation flux are consistent between GiOcean and IMERG. While consistent there isn't a particularly strong overall trend in precipitation in either study region (Figure 4gh). Given the overall magnitude of precipitation flux in these regions (Figure 1h), this points to a fairly large interannual variability in the precipitation flux demand by the atmosphere that makes it difficult to disentangle meteorological and aerosol driving of cloud macrophysical properties as well as scavenging of cloud droplet number (Wood et al., 2012; Kang et al., 2022). In the following section we attempt to disentangle these factors with a set of simple source-sink models of cloud droplet number and cloud liquid mass.

295 3.3 Source-sink models of cloud microphysics and macrophysics

As outlined above, GiOcean generally replicates spatial and temporal patterns of AOD and precipitation rate (Figure 1, 3, and 4). The correspondence between GiOcean and observations regarding cloud microphysics and macrophysics (i.e. Nd and LWP) is less robust. Understanding the sources of these biases and whether this points towards issues related to how liquid clouds in GiOcean respond to aerosols or how they respond to the moisture demands from the large scale environment requires partitioning their behavior into those factors. Here, we consider cloud droplet number and cloud liquid mass in terms a simple source-sink approximate steady state model to evaluate monthly patterns of both quantities in the outflow regions identified in Figure 1.

The source sink model of Nd is based on Wood et al. (2012), which represents the steady state Nd as a function of activation of CCN into Nd from free tropospheric sources and removal of Nd through precipitation. In Wood et al. (2012), the steady state model was explicitly adapted for airborne observations and was able to show that the gradient of Nd off the coast of Peru was mostly due to increasing precipitation sinks as opposed to decreasing CCN sources. Here we do not have the same data available and instead of characterizing Nd in terms of precipitation rates estimated from radar reflectivity and airborne in-situ CCN measurements we characterize it in terms of precipitation rate and AOD (Figure 5). While these terms are imperfect analogs to CCN near cloud and coalescence scavenging in cloud, we can compare GiOcean to spaceborne observations of these quantities.

The dependence of Nd on AOD and precipitation rate for each outflow region and for GiOcean and observations is shown in Figure 5. We don't expect Nd to depend linearly on either AOD or precipitation rate (Wood et al., 2012), so we formulate our source-sink model as a look up table. Due to the large range and log-normal distributions of precipitation rate and AOD we use logarithmic bins.

In both observations and GiOcean the range of precipitation rate and AOD in the North American outflow region is much smaller than in East Asia (Figure 5). AOD is nearly an order of magnitude lower with a smaller range in the North American outflow region in both observations and GiOcean. However, within the data available from observations the pattern of Nd as a function of AOD and precipitation rate from observations is similar to GiOcean in East Asian with increasing Nd in response to AOD and decreasing Nd in response to precipitation, consistent with the expected behavior in response to sources and sinks



320 (Figure 5ac). There is a less pronounced but similar behavior in the pristine North American outflow apparent in GiOcean, but not in observations (Figure 5bd).

Overall, the dependence of Nd on AOD and precipitation rate inferred from the compositing in Figure 1 is consistent with our a priori expectations based on Wood et al. (2012). Increasing precipitation removes droplets via coalescence scavenging, resulting in a decrease in Nd with increasing precipitation rate. Increasing AOD corresponds to an increase in CCN-relevant aerosol and an increasing in Nd. This behavior is clearer in GiOcean than in observations. The larger data volume and greater range of AOD and precipitation rate in the East Asian outflow makes this pattern more apparent in this region. This may indicate that the dependence of Nd on sources and sinks in GiOcean is too strong, which is consistent with the strong off-coastal gradients in Nd Figure 1d compared to observations in Figure 1c. Of course, it may also be due to imperfect observations of Nd, AOD, and precipitation rate relative to the output from GiOcean which provides an exact representation of these quantities in the reanalysis grid.

The simple source-sink model of LWP is based on previous work examining extratropical ACI in the context of the precipitation rate imposed by the large-scale moisture convergence (McCoy et al., 2020a, 2018b). In turn, the amount of cloud dictated by the precipitation rate is set by the precipitation efficiency of the cloud. One determinant of precipitation efficiency is the cloud droplet number (Song et al., 2024; Khairoutdinov and Kogan, 2000; Albrecht, 1989). In this context, we composite LWP on Nd and precipitation rate (Figure 6). Overall, the dependence of LWP on Nd and precipitation rate follows our a priori expectation. In both regions and in observations and GiOcean LWP increased with precipitation rate in keeping with a greater removal rate of converging moisture by clouds. In both regions in GiOcean (Figure 6ab), LWP increased with Nd due to decreased precipitation efficiency, which retains more liquid cloud amount, while this behavior is less apparent in observations (Figure 6cd). Similarly to Figure 5, the range of LWP in the North American outflow region is smaller than in East Asia. The observed dependence of LWP on Nd is much weaker than predicted by GiOcean. This may indicate that the effects of precipitation suppression may be too strong in GiOcean.

To answer the question of how these inferred dependencies translate to trends in cloud microphysics and macrophysics we used the look up tables from Figure 5 and Figure 6 to predict the decadal trends of Nd and LWP for GiOcean and observations over the study regions. Sensitivity tests are applied for the look up tables by setting AOD, Nd, precipitation rate to a constant value and letting all other terms vary (Figure 7, 8) to understand the relative importance of sources and sinks on temporal variations of Nd and LWP.

We examined the proportion of variance in the annual means of Nd explained by the look up table (Figure 5) when given precipitation rate and AOD and when setting AOD and precipitation rate a constant, respectively. For both GiOcean and observations, the Nd look up table mostly captures the decadal trend of Nd over East Asia and North America outflow regions when the look up table uses a fixed precipitation rate, with an explained variance of Nd annual means by Nd look up table predictions with fixed precipitation rate greater than 94%. However, with fixed AOD, the Nd look up table model is unable to reproduce the decadal trend of Nd (Figure 7 abcd) with an explained variance of Nd annual means by look up table predictions with a fixed AOD less than 25%. This suggests that the temporal variations in Nd is largely driven by aerosol (as encapsulated by the AOD) and is consistent between GiOcean and observations in both East Asia and North America regions. This is in



355 contrast to Nd spatial variations where a stronger gradient in precipitation rate away from coasts in GiOcean compared with observations is accompanied with sharper decrease in Nd in GiOcean. However, this is consistent with the findings in Wood et al. (2012) that precipitation drives droplet concentration variability spatially in marine liquid clouds. Overall, precipitation scavenging on Nd is too strong in GiOcean compared with observations (Figure 1bd and 5).

The look up table for LWP (Figure 6) was able to reproduce the observed LWP trend in the East Asia and North America
360 outflow regions with fixed precipitation rate in GiOcean. 74% of the variability in LWP annual means is explained by LWP annual means predicted with a constant precipitation rate in the East Asia outflow region, and 49% in the North America outflow region. However, the look up table is unable to capture the LWP trend when forcing the Nd a constant in both outflow regions in GiOcean (Figure 8ab). Correlation between LWP annual means and the LWP annual means predicted with a constant Nd is close to 0 in the East Asia outflow region in GiOcean (Figure 8a), indicating Nd drives the most of LWP temporal variation by
365 precipitation suppression effect in the East Asia outflow region in GiOcean. In the North America outflow region in GiOcean (Figure 8b), the correlation coefficients between LWP annual means with scenarios of either setting precipitation rate or Nd a constant are both positive and are greater than 0.5. In other words, both Nd and precipitation rate temporal variations contribute to LWP decadal trend, while Nd drives the majority of LWP temporal variation by precipitation suppression effect with a larger correlation coefficient of 0.7, while large scale precipitation scavenging plays a small role in LWP decadal trend in the North
370 America outflow region in GiOcean. In contrast to GiOcean, the decadal trend of observations from MAC-LWP is largely caused by variations in IMERG precipitation in the East Asia and North America outflow regions (Figure 8cd). This indicates the precipitation suppression effect induced by Nd variation is too strong in GiOcean compared with observations in both regions.

4 Conclusions

375 Global climate models have implemented two-moment cloud microphysics scheme and achieved more realistic representation of clouds (Ghan et al., 1997; Lohmann et al., 1999; Ming et al., 2007; Barahona et al., 2014b; Morrison and Gettelman, 2008), but until now reanalyses have not included two-moment microphysics coupled to aerosols. In this study, we evaluate the new GiOcean reanalysis with two-moment cloud microphysics against satellite retrievals.

To evaluate ACI in warm clouds in GiOcean, we first compare variables important for ACI from GiOcean with available
380 spaceborne remote sensing in terms of spatial and temporal variability. The GiOcean is in good agreement with MODIS AOD and IMERG precipitation overall but with lower AOD in GiOcean in the Southern Ocean and areas of substantial effusive volcanic emissions. The correspondence between GiOcean and observations regarding Nd and LWP is less robust (Figure 1,2,3,4).

A key question in GiOcean is whether the addition of two-moment cloud microphysics has created aerosol-cloud adjustments
385 that are realistic. This is difficult to do because of the causally-ambiguous nature of aerosol-cloud adjustments (McCoy et al., 2020a; Gryspeerdt et al., 2019). The majority of variability in cloud macrophysical properties (i.e. LWP) is driven by variations in the meteorological state of the atmosphere, not the microphysical state of the clouds (i.e. Nd) (Wall et al., 2022; Bender et al.,



2019; McCoy et al., 2018b). In terms of understanding aerosol-cloud adjustments through precipitation suppression, the key driver of this behavior has been argued to be precipitation rate (McCoy et al., 2020a). While less complex, Nd also suffers from some degree of causal ambiguity and the primary driver of spatial patterns of Nd is found to be precipitation rather than aerosol (Wood et al., 2012; Kang et al., 2022). This means that errors in cloud properties may be dominated by errors in how meteorology and large-scale moisture convergence translates to precipitation rate.

To tackle attribution of liquid cloud properties to ACI we put forward simple models of liquid cloud microphysical and macrophysical properties. We expect that the relationships between sources, sinks, and state variables will be non-linear (Wood et al., 2012; McCoy et al., 2018b) and we build up look up tables of both microphysical and macrophysical liquid cloud state variables. These are: Nd (microphysical state variable) as a function of precipitation rate (sink) and AOD (source); and LWP (macrophysical state variable) as a function of precipitation rate (sink) and Nd (source).

Our framework allows us to characterize Nd variability in terms of sources and sinks (Wood et al., 2012). As expected, larger AOD corresponds to larger Nd and shows that aerosol and cloud properties are linked through aerosol activation. This behavior is clearer in GiOcean than in observation and suggests that Nd in GiOcean is too strongly dependent on sources and sink compared to observations (Figure 6).

Similarly, we examine the dependence of LWP on Nd as a function of the sink enforced by precipitation rate. Larger Nd corresponds to larger LWP at fixed precipitation rate consistent with the implementation of two-moment cloud microphysics and precipitation suppression in GiOcean (Figure 6). Broadly, the dependence of LWP on Nd appears to be more pronounced in GiOcean than observations, suggesting that aerosol-cloud adjustments through precipitation suppression may be too active in GiOcean.

Ultimately, in terms of understanding climate we are concerned with the cloud response to long-term changes in emissions (McCoy et al., 2018a; Wall et al., 2022). We find that GiOcean is able to predict decadal trends in AOD and Nd off the coasts of the Peoples Republic of China and the United State of America (Figure 4abcd). We leverage this to both test our look up tables of Nd and LWP derived from observations and GiOcean and use them for attribution. To do this we fix source and sink terms once at a time. Temporal variations in Nd in GiOcean and observations in outflow regions are dominated by AOD and the attributed variation to this term is consistent between observations and GiOcean (Figure 7). Variations in LWP in GiOcean is largely driven by Nd variation through precipitation suppression off the coasts of the Peoples Republic of China and the United State of America (the fixed Nd and full look up table prediction are far apart), in contrast to observations which driven by the precipitation sink term (Figure 8; the fixed Nd and full look up table predictions are relatively close together compared to the fixed precipitation rate prediction).

In summary, GiOcean's climatology of aerosol and liquid cloud properties compares favorably to observations (Figure 1 and 2). Analysis of GiOcean in the context of a simple source-sink model of ACI shows that the two-moment cloud microphysics scheme in GiOcean (i) represents the activation of aerosol into cloud droplets (Figure 5) and (ii) represents precipitation suppression due to enhanced aerosol (Figure 6). However, we find that the dependence of cloud droplets on aerosol and removal of cloud droplets by precipitation may be too strong in GiOcean compared with spaceborne remote sensing observations. We also find that the precipitation suppression effect in GiOcean might be too strong (Figure 8b). Nevertheless, GiOcean is the only



reanalysis to date that explicitly includes aerosol-cloud interactions, and we expect it to significantly advance our understanding of the critical, yet still poorly understood role of ACI on climate, particularly on decadal time scales.

425

Data availability. Data assimilation for GiOcean reanalysis is based on the Global Earth System Model Subseasonal-to-Seasonal (GEOS-S2S) prediction system and is described in detail in Molod et al. (2020b). Table 1 of Molod et al. (2020a) summarizes the various in situ profile observations used for data assimilation. Aerosol assimilation uses the Goddard Aerosol Assimilation System (GAAS). The aerosol optical depth (AOD), is assimilated using the observing system described in Table 2 of Randles et al. (2017). The atmosphere component of GiOcean is replayed to GEOS-IT which assimilates all the datasets used in MERRA-2 (Gelaro et al., 2017a).

GiOcean dataset is on its way to become public at <https://portal.nccs.nasa.gov/datashare/>. This is a temporary repository we will use to share the GiOcean data, but it would likely be moved to a more permanent location eventually.

435

Author contributions.

CS and DTM applied the methodology and generated the results. CS, DTM and DB contributed to the analysis and interpretation of results and wrote the article. DB and AM participated in the development of GiOcean reanalysis dataset.

Competing interests. The authors declare that they have no conflict of interest.



Acknowledgements. CS and DTM were supported by NASA Grant 80NSSC21K2014 and DTM was supported by the U.S. Department of Energy's Atmospheric System Research Federal Award DE-SC002227; U.S. Department of Energy's Established Program to Stimulate Competitive Research DE-SC0024161; U.S. Department of Energy's Earth and Environmental System Modeling DE-SC0025208; and NASA Precipitation Measurement Mission Science Team Grant 80NSSC22K0609. DB was supported by the NASA Modeling, Analysis and Prediction program, Grant NNH20ZDA001N-MAP.



References

- Abdul-Razzak, H. and Ghan, S.: A parameterization of aerosol activation, 2. Multiple aerosol types., *J. Geophys. Res.*, 105, 6837–6844, doi:10.1029/1999JD901161, 2000.
- 450 Ackerman, A. S., Kirkpatrick, M. P., Stevens, D. E., and Toon, O. B.: The impact of humidity above stratiform clouds on indirect aerosol climate forcing, *Nature*, 432, 1014–1017, <https://doi.org/10.1038/nature03174>, 2004.
- Albrecht, B. A.: Aerosols, Cloud Microphysics, and Fractional Cloudiness, *Science*, 245, 1227–1230, <https://doi.org/10.1126/science.245.4923.1227>, 1989.
- 455 Balmes, K., Fu, Q., and Thorsen, T.: The diurnal variation of the aerosol optical depth at the ARM SGP site, *Earth and Space Science*, 8, e2021EA001852, 2021.
- Bangert, M., Nenes, A., Vogel, B., Vogel, H., Barahona, D., Karydis, V. A., Kumar, P., Kottmeier, C., and Blahak, U.: Saharan dust event impacts on cloud formation and radiation over Western Europe, *Atmospheric Chemistry and Physics*, 12, 4045–4063, <https://doi.org/10.5194/acp-12-4045-2012>, 2012.
- 460 Barahona, D. and Nenes, A.: Parameterizing the competition between homogeneous and heterogeneous freezing in cirrus cloud formation - polydisperse ice nuclei, *Atmospheric Chemistry & Physics*, 9, 5933–5948, <https://doi.org/10.5194/acp-9-5933-2009>, 2009.
- Barahona, D., Molod, A., Bacmeister, J., Nenes, A., Gettelman, A., Morrison, H., Phillips, V., and Eichmann, A.: Development of two-moment cloud microphysics for liquid and ice within the NASA Goddard Earth Observing System Model (GEOS-5), *Geosc. Model Dev.*, 7, 1733–1766, <https://doi.org/10.5194/gmd-7-1733-2014>, 2014a.
- 465 Barahona, D., Molod, A., Bacmeister, J., Nenes, A., Gettelman, A., Morrison, H., Phillips, V., and Eichmann, A.: Development of two-moment cloud microphysics for liquid and ice within the NASA Goddard Earth Observing System Model (GEOS-5), *Geoscientific Model Development*, 7, 1733–1766, 2014b.
- Barahona, D., Molod, A., and Kalesse, H.: Direct estimation of the global distribution of vertical velocity within cirrus clouds, *Scientific Reports*, 7, 6840, <https://doi.org/10.1038/s41598-017-07038-6>, 2017.
- 470 Bellouin, N., Quaas, J., Gryspeerdt, E., Kinne, S., Stier, P., Watson-Parris, D., Boucher, O., Carslaw, K. S., Christensen, M., Daniau, A.-L., Dufresne, J.-L., Feingold, G., Fiedler, S., Forster, P., Gettelman, A., Haywood, J. M., Lohmann, U., Malavelle, F., Mauritsen, T., McCoy, D. T., Myhre, G., Mülmenstädt, J., Neubauer, D., Possner, A., Rugenstein, M., Sato, Y., Schulz, M., Schwartz, S. E., Sourdeval, O., Storelvmo, T., Toll, V., Winker, D., and Stevens, B.: Bounding Global Aerosol Radiative Forcing of Climate Change, *Reviews of Geophysics*, 58, <https://doi.org/10.1029/2019rg000660>, 2019.
- 475 Bellucci, A., Haarsma, R., Bellouin, N., Booth, B., Cagnazzo, C., van den Hurk, B., Keenlyside, N., Koenigk, T., Massonnet, F., Matera, S., et al.: Advancements in decadal climate predictability: The role of nonoceanic drivers, *Reviews of Geophysics*, 53, 165–202, 2015.
- Bender, F.-M., Frey, L., McCoy, D. T., Grosvenor, D. P., and Mohrmann, J. K.: Assessment of aerosol–cloud–radiation correlations in satellite observations, climate models and reanalysis, *Climate Dynamics*, 52, 4371–4392, 2019.
- Benedetti, A. and Vitart, F.: Can the direct effect of aerosols improve subseasonal predictability?, *Monthly Weather Review*, 146, 3481–3498, 480 2018.
- Bennartz, R., Fan, J., Rausch, J., Leung, L. R., and Heidinger, A. K.: Pollution from China increases cloud droplet number, suppresses rain over the East China Sea, *Geophysical Research Letters*, 38, n/a–n/a, <https://doi.org/10.1029/2011gl047235>, 2011.
- Board, O. S., National Academies of Sciences, E., Medicine, et al.: Next generation earth system prediction: strategies for subseasonal to seasonal forecasts, National Academies Press, 2016.



- 485 Bozzo, A., Benedetti, A., Flemming, J., Kipling, Z., and Remy, S.: An aerosol climatology for global models based on the tropospheric aerosol scheme in the Integrated Forecasting System of ECMWF, *Geoscientific Model Development*, 13, 1007–1034, 2020.
- Breen, K., Barahona, D., Yuan, T., Bian, H., and C, J. S.: Effect of volcanic emissions on clouds during the 2008 and 2018 Kilauea degassing events, *Atmos. Chem. Phys.*, p. Submitted, 2020.
- Breen, K. H., Barahona, D., Yuan, T., Bian, H., and James, S. C.: Effect of volcanic emissions on clouds during the 2008 and 2018 Kilauea
490 degassing events, *Atmospheric Chemistry and Physics*, 21, 7749–7771, <https://doi.org/10.5194/acp-21-7749-2021>, 2021.
- Bretherton, C. S., Blossey, P. N., and Uchida, J.: Cloud droplet sedimentation, entrainment efficiency, and subtropical stratocumulus albedo, *Geophysical Research Letters*, 34, <https://doi.org/10.1029/2006gl027648>, 2007.
- Buchard, V., Da Silva, A., Randles, C., Colarco, P., Ferrare, R., Hair, J., Hostetler, C., Tackett, J., and Winker, D.: Evaluation of the surface PM_{2.5} in Version 1 of the NASA MERRA Aerosol Reanalysis over the United States, *Atmospheric Environment*, 125, 100–111, 2016a.
- 495 Buchard, V., Da Silva, A., Randles, C., Colarco, P., Ferrare, R., Hair, J., Hostetler, C., Tackett, J., and Winker, D.: Evaluation of the surface PM_{2.5} in Version 1 of the NASA MERRA Aerosol Reanalysis over the United States, *Atmospheric Environment*, 125, 100–111, <https://doi.org/10.1016/j.atmosenv.2015.11.004>, 2016b.
- Carn, S., Fioletov, V., McLinden, C., Li, C., and Krotkov, N.: A decade of global volcanic SO₂ emissions measured from space, *Scientific reports*, 7, 44 095, <https://doi.org/10.1038/srep44095>, 2017a.
- 500 Carn, S. A., Fioletov, V. E., McLinden, C. A., Li, C., and Krotkov, N. A.: A decade of global volcanic SO₂ emissions measured from space, *Scientific Reports*, 7, 44 095, <https://doi.org/10.1038/srep44095> <https://www.nature.com/articles/srep44095#supplementary-information>, 2017b.
- Colarco, P. R., Nowottnick, E. P., Randles, C. A., Yi, B., Yang, P., Kim, K.-M., Smith, J. A., and Colarco, N. F.: Impact of radiatively interactive dust aerosols in the NASA GEOS-5 climate model: Sensitivity to dust particle shape and refractive index, *Journal of Geophysical Research: Atmospheres*, 115, D23 203, <https://doi.org/10.1029/2010JD014471>, 2010.
- 505 Ekman, A. M.: Aerosols and their seasonal variability-Are aerosols important for seasonal prediction?, *ECMWF Seminar on Seasonal Prediction*, 2012.
- Ekman, A. M.: Do sophisticated parameterizations of aerosol-cloud interactions in CMIP5 models improve the representation of recent observed temperature trends?, *Journal of Geophysical Research: Atmospheres*, 119, 817–832, 2014.
- 510 Elsaesser, G. S., O’Dell, C. W., Lebsock, M. D., Bennartz, R., Greenwald, T. J., and Wentz, F. J.: The Multi-Sensor Advanced Climatology of Liquid Water Path (MAC-LWP), *Journal of Climate*, 0, null, <https://doi.org/10.1175/jcli-d-16-0902.1>, 2017.
- Fan, J., Wang, Y., Rosenfeld, D., and Liu, X.: Review of aerosol–cloud interactions: Mechanisms, significance, and challenges, *Journal of the Atmospheric Sciences*, 73, 4221–4252, 2016.
- Field, P. R. and Furtado, K.: How biased is aircraft cloud sampling?, *Journal of Atmospheric and Oceanic Technology*, 33, 185–189, 2016.
- 515 Gelaro, R., McCarty, W., Suárez, M. J., Todling, R., Molod, A., Takacs, L., Randles, C. A., Darmenov, A., Bosilovich, M. G., Reichle, R., et al.: The modern-era retrospective analysis for research and applications, version 2 (MERRA-2), *Journal of climate*, 30, 5419–5454, 2017a.
- Gelaro, R., McCarty, W., Suárez, M. J., Todling, R., Molod, A., Takacs, L., Randles, C. A., Darmenov, A., Bosilovich, M. G., Reichle, R., Wargan, K., Coy, L., Cullather, R., Draper, C., Akella, S., Buchard, V., Conaty, A., da Silva, A. M., Gu, W., Kim, G.-K., Koster, R.,
520 Lucchesi, R., Merkova, D., Nielsen, J. E., Partyka, G., Pawson, S., Putman, W., Rienecker, M., Schubert, S. D., Sienkiewicz, M., and Zhao, B.: The Modern-Era Retrospective Analysis for Research and Applications, Version 2 (MERRA-2), *Journal of Climate*, 30, 5419–5454, <https://doi.org/10.1175/JCLI-D-16-0758.1>, 2017b.



- Ghan, S. J., Leung, L. R., Easter, R. C., and Abdul-Razzak, H.: Prediction of cloud droplet number in a general circulation model, *Journal of Geophysical Research: Atmospheres*, 102, 21 777–21 794, 1997.
- 525 Gordon, H., Kirkby, J., Baltensperger, U., Bianchi, F., Breitenlechner, M., Curtius, J., Dias, A., Dommen, J., Donahue, N. M., Dunne, E. M., Duplissy, J., Ehrhart, S., Flagan, R. C., Frege, C., Fuchs, C., Hansel, A., Hoyle, C. R., Kulmala, M., Kürten, A., Lehtipalo, K., Makhmutov, V., Molteni, U., Rissanen, M. P., Stozkhov, Y., Tröstl, J., Tsagkogeorgas, G., Wagner, R., Williamson, C., Wimmer, D., Winkler, P. M., Yan, C., and Carslaw, K. S.: Causes and importance of new particle formation in the present-day and preindustrial atmospheres, *Journal of Geophysical Research: Atmospheres*, 122, 8739–8760, <https://doi.org/10.1002/2017JD026844>, 2017.
- 530 Griffies, S. M.: Elements of the Modular Ocean Model (MOM), GFDL Ocean Group Technical Report No. 7, 2012.
- Griffies, S. M., Biastoch, A., Böning, C. W., Bryan, F. O., Danabasoglu, G., Chassignet, E. P., England, M. H., Gerdes, R., Haak, H., Hallberg, R. W., Hazeleger, W., Jungclaus, J. H., Large, W. G., Madec, G., Pirani, A., Samuels, B. L., Scheinert, M., Gupta, A. S., Severijns, C., Simmons, H. L., Treguier, A. M., Winton, M., Yeager, S. G., and Yin, J.: Formulation of an ocean model for global climate simulations, *Ocean Science*, 1, 45–79, <https://doi.org/10.5194/os-1-45-2005>, 2005.
- 535 Grosvenor, D. and Wood, R.: The effect of solar zenith angle on MODIS cloud optical and microphysical retrievals within marine liquid water clouds, *Atmospheric Chemistry and Physics*, 14, 7291–7321, 2014a.
- Grosvenor, D. P. and Wood, R.: The effect of solar zenith angle on MODIS cloud optical and microphysical retrievals within marine liquid water clouds, *Atmospheric Chemistry & Physics*, 14, 7291–7321, <https://doi.org/10.5194/acp-14-7291-2014>, 2014b.
- Grosvenor, D. P., Sourdeval, O., Zuidema, P., Ackerman, A., Alexandrov, M. D., Bennartz, R., Boers, R., Cairns, B., Chiu, J. C., Christensen, M., Deneke, H., Diamond, M., Feingold, G., Fridlind, A., Hünerbein, A., Knist, C., Kollias, P., Marshak, A., McCoy, D., Merk, D., Painemal, D., Rausch, J., Rosenfeld, D., Russchenberg, H., Seifert, P., Sinclair, K., Stier, P., van Diedenhoven, B., Wendisch, M., Werner, F., Wood, R., Zhang, Z., and Quaas, J.: Remote Sensing of Droplet Number Concentration in Warm Clouds: A Review of the Current State of Knowledge and Perspectives, *Reviews of Geophysics*, 56, 409–453, <https://doi.org/10.1029/2017rg000593>, 2018.
- 540 Gryspeerdt, E., Goren, T., Sourdeval, O., Quaas, J., Mülmenstädt, J., Dipu, S., Unglaub, C., Gettelman, A., and Christensen, M.: Constraining the aerosol influence on cloud liquid water path, *Atmospheric Chemistry & Physics*, 19, 5331–5347, <https://doi.org/10.5194/acp-19-5331-2019>, 2019.
- Gryspeerdt, E., McCoy, D. T., Crosbie, E., Moore, R. H., Nott, G. J., Painemal, D., Small-Griswold, J., Sorooshian, A., and Ziemba, L.: The impact of sampling strategy on the cloud droplet number concentration estimated from satellite data, *Atmos. Meas. Tech.*, 15, 3875–3892, <https://doi.org/10.5194/amt-15-3875-2022>, publisher: Copernicus Publications, 2022.
- 550 Hill, C., DeLuca, C., Balaji, V., Suarez, M., and da Silva, A.: The architecture of the Earth System Modeling Framework, *Computing in Science Engineering*, 6, 18–28, <https://doi.org/10.1109/MCISE.2004.1255817>, 2004.
- Huffman, G. J., Bolvin, D. T., Braithwaite, D., Hsu, K.-L., Joyce, R. J., Kidd, C., Nelkin, E. J., Sorooshian, S., Stocker, E. F., Tan, J., Wolff, D. B., and Xie, P.: Integrated Multi-satellite Retrievals for the Global Precipitation Measurement (GPM) Mission (IMERG), in: *Satellite Precipitation Measurement: Volume 1*, edited by Levizzani, V., Kidd, C., Kirschbaum, D. B., Kummerow, C. D., Nakamura, K., and Turk, F. J., pp. 343–353, Springer International Publishing, Cham, ISBN 978-3-030-24568-9, https://doi.org/10.1007/978-3-030-24568-9_19, 2020.
- 555 Huffman, G. J., Bolvin, D. T., Joyce, R., Kelley, O. A., Nelkin, E. J., Portier, A., Stocker, E. F., Tan, J., Watters, D. C., and West, B. J.: IMERG V07 Release Notes, 2023.
- Hunke, E. C.: Sea ice component of the Community Ice CodE (CICE), Version 4, Los Alamos National Laboratory Tech. Rep. LA-CC-06-560 012, 2008.



- IPCC: Climate Change 2013: The Physical Science Basis. Contribution of Working Group I to the Fifth Assessment Report of the Intergovernmental Panel on Climate Change, Cambridge University Press, Cambridge, United Kingdom and New York, NY, USA, ISBN 978-1-107-66182-0, 2013.
- Jin, H. and Nasiri, S. L.: Evaluation of AIRS cloud-thermodynamic-phase determination with CALIPSO, *Journal of Applied Meteorology and Climatology*, 53, 1012–1027, 2014.
- 565 Kang, L., Marchand, R. T., Wood, R., and McCoy, I. L.: Coalescence Scavenging Drives Droplet Number Concentration in Southern Ocean Low Clouds, *Geophysical Research Letters*, n/a, e2022GL097819, <https://doi.org/10.1029/2022GL097819>, publisher: John Wiley & Sons, Ltd, 2022.
- Kasibhatla, P., Chameides, W., and John, J. S.: A three-dimensional global model investigation of seasonal variations in the atmospheric burden of anthropogenic sulfate aerosols, *Journal of Geophysical Research: Atmospheres*, 102, 3737–3759, 1997.
- 570 Khairoutdinov, M. and Kogan, Y.: A new cloud physics parameterization in a large-eddy simulation model of marine stratocumulus, *Monthly weather review*, 128, 229–243, 2000.
- Koster, R. D., Suarez, M. J., Ducharne, A., Stieglitz, M., and Kumar, P.: A catchment-based approach to modeling land surface processes in a GCM: 1. Model structure, *Journal of Geophysical Research: Atmospheres*, 105, 24 809–24 822, <https://doi.org/10.1029/2000JD900327>,
- 575 2000.
- Lohmann, U., Feichter, J., Chuang, C. C., and Penner, J. E.: Prediction of the number of cloud droplets in the ECHAM GCM, *Journal of Geophysical Research: Atmospheres*, 104, 9169–9198, 1999.
- McCoy, D., Bender, F.-M., Mohrmann, J., Hartmann, D., Wood, R., and Grosvenor, D.: The global aerosol-cloud first indirect effect estimated using MODIS, MERRA, and AeroCom, *Journal of Geophysical Research: Atmospheres*, 122, 1779–1796, 2017.
- 580 McCoy, D. T., Bender, F. A. M., Grosvenor, D. P., Mohrmann, J. K., Hartmann, D. L., Wood, R., and Field, P. R.: Predicting decadal trends in cloud droplet number concentration using reanalysis and satellite data, *Atmospheric Chemistry and Physics*, 18, 2035–2047, <https://doi.org/10.5194/acp-18-2035-2018>, 2018a.
- McCoy, D. T., Field, P. R., Schmidt, A., Grosvenor, D. P., Bender, F. A. M., Shipway, B. J., Hill, A. A., Wilkinson, J. M., and Elsaesser, G. S.: Aerosol midlatitude cyclone indirect effects in observations and high-resolution simulations, *Atmospheric Chemistry and Physics*,
- 585 18, 5821–5846, <https://doi.org/10.5194/acp-18-5821-2018>, 2018b.
- McCoy, D. T., Field, P., Gordon, H., Elsaesser, G. S., and Grosvenor, D. P.: Untangling causality in midlatitude aerosol–cloud adjustments, *Atmospheric Chemistry and Physics*, 20, 4085–4103, <https://doi.org/10.5194/acp-20-4085-2020>, 2020a.
- McCoy, I. L., McCoy, D. T., Wood, R., Regayre, L., Watson-Parris, D., Grosvenor, D. P., Mulcahy, J. P., Hu, Y., Bender, F. A. M., Field, P. R., Carslaw, K. S., and Gordon, H.: The hemispheric contrast in cloud microphysical properties constrains aerosol forcing, *Proceedings of the National Academy of Sciences*, p. 201922502, <https://doi.org/10.1073/pnas.1922502117>, 2020b.
- 590 McCoy, I. L., Bretherton, C. S., Wood, R., Twohy, C. H., Gettelman, A., Bardeen, C. G., and Toohey, D. W.: Influences of Recent Particle Formation on Southern Ocean Aerosol Variability and Low Cloud Properties, *Journal of Geophysical Research: Atmospheres*, 126, e2020JD033 529, <https://doi.org/10.1029/2020JD033529>, publisher: John Wiley & Sons, Ltd, 2021.
- Michibata, T. and Takemura, T.: Evaluation of autoconversion schemes in a single model framework with satellite observations, *Journal of Geophysical Research: Atmospheres*, 120, 9570–9590, <https://doi.org/10.1002/2015JD023818>, _eprint: <https://agupubs.onlinelibrary.wiley.com/doi/pdf/10.1002/2015JD023818>, 2015.
- 595 Mikkelsen, A.: Constraining Aerosol-Cloud Adjustments With Surface Observations, Master’s thesis, University of Wyoming, United States – Wyoming, <https://www.libproxy.uwyo.edu/login?url=https://www.proquest.com/dissertations-theses/>



- constraining-aerosol-cloud-adjustments-with/docview/3057539218/se-2?accountid=14793, iISBN: 9798382724621 Publication Title:
600 ProQuest Dissertations and Theses 31242366, 2024.
- Ming, Y., Ramaswamy, V., Donner, L. J., Phillips, V. T., Klein, S. A., Ginoux, P. A., and Horowitz, L. W.: Modeling the interactions between aerosols and liquid water clouds with a self-consistent cloud scheme in a general circulation model, *Journal of the atmospheric sciences*, 64, 1189–1209, 2007.
- Molod, A., Takacs, L., Suarez, M., and Bacmeister, J.: Development of the GEOS-5 Atmospheric General Circulation Model: Evolution
605 from MERRA to MERRA2, *Geoscientific Model Development*, 8, 1339–1356, <https://doi.org/10.5194/gmd-8-1339-2015>, 2015.
- Molod, A., Hackert, E., Vikhliayev, Y., Zhao, B., Barahona, D., Vernieres, G., Borovikov, A., Kovach, R. M., Marshak, J., Schubert, S., Li, Z., Lim, Y.-K., Andrews, L. C., Cullather, R., Koster, R., Achuthavarier, D., Carton, J., Coy, L., Friere, J. L. M., Longo, K. M., Nakada, K., and Pawson, S.: GEOS-S2S Version 2: The GMAO High-Resolution Coupled Model and Assimilation System for Seasonal Prediction, *J. Geophys. Res. Atmos.*, 125, 2020a.
- 610 Molod, A., Hackert, E., Vikhliayev, Y., Zhao, B., Barahona, D., Vernieres, G., Borovikov, A., Kovach, R. M., Marshak, J., Schubert, S., et al.: GEOS-S2S version 2: The GMAO high-resolution coupled model and assimilation system for seasonal prediction, *Journal of Geophysical Research: Atmospheres*, 125, e2019JD031767, <https://doi.org/10.1029/2019JD031767>, 2020b.
- Morcrette, J.-J., Benedetti, A., Ghelli, A., Kaiser, J., and Tompkins, A.: Aerosol-cloud-radiation interactions and their impact on ECMWF/MACC forecasts, *European Centre for Medium-Range Weather Forecasts*, 2011.
- 615 Morrison, H. and Gettelman, A.: A new two-moment bulk stratiform cloud microphysics scheme in the Community Atmosphere Model, version 3 (CAM3). Part I: Description and numerical tests, *Journal of Climate*, 21, 3642–3659, 2008.
- Mulcahy, J. P., Jones, C., Sellar, A., Johnson, B., Boutle, I. A., Jones, A., Andrews, T., Rumbold, S. T., Mollard, J., Bellouin, N., Johnson, C. E., Williams, K. D., Grosvenor, D. P., and McCoy, D. T.: Improved Aerosol Processes and Effective Radiative Forcing in HadGEM3 and UKESM1, *Journal of Advances in Modeling Earth Systems*, 0, <https://doi.org/10.1029/2018MS001464>, 2018.
- 620 Nakajima, T. and King, M. D.: Determination of the optical thickness and effective particle radius of clouds from reflected solar radiation measurements. Part I: Theory, *J. Atmos. Sci.*, 47, 1878–1893, 1990.
- Nowotnick, E., Colarco, P., Braun, S., Barahona, D., da Silva, A., Hlavka, D., McGill, M., and Spackman, J.: Dust impacts on the 2012 Hurricane Nadine track during the NASA HS3 field campaign, *Journal of the atmospheric sciences*, 75, 2473–2489, 2018.
- O’Dell, C. W., Wentz, F. J., and Bennartz, R.: Cloud liquid water path from satellite-based passive microwave observations: A new climatol-
625 ogy over the global oceans, *Journal of Climate*, 21, 1721–1739, 2008.
- Penny, S. G., Miyoshi, T., and Kalnay, E.: Localization of the ensemble transform Kalman filter, *Monthly Weather Review*, 141, 1601–1621, <https://doi.org/10.1175/MWR-D-12-00091.1>, 2013.
- Pradhan, R. K. and Markonis, Y.: Performance evaluation of GPM IMERG precipitation products over the tropical oceans using Buoys, *Journal of Hydrometeorology*, 24, 1755–1770, 2023.
- 630 Randles, C. A., da Silva, A. M., Buchard, V., Colarco, P. R., Darmenov, A., Govindaraju, R., Smirnov, A., Holben, B., Ferrare, R., Hair, J., Shinozuka, Y., and Flynn, C. J.: The MERRA-2 Aerosol Reanalysis, 1980 Onward. Part I: System Description and Data Assimilation Evaluation, *Journal of Climate*, 30, 6823–6850, <https://doi.org/10.1175/JCLI-D-16-0609.1>, 2017.
- Reale, O., Lau, K., Da Silva, A., and Matsui, T.: Impact of assimilated and interactive aerosol on tropical cyclogenesis, *Geophysical research letters*, 41, 3282–3288, 2014.



- 635 Regayre, L. A., Deaconu, L., Grosvenor, D. P., Sexton, D. M., Symonds, C., Langton, T., Watson-Paris, D., Mulcahy, J. P., Pringle, K. J., Richardson, M., et al.: Identifying climate model structural inconsistencies allows for tight constraint of aerosol radiative forcing, *Atmospheric Chemistry and Physics*, 23, 8749–8768, 2023.
- Rienecker, M. M., Suarez, M. J., Todling, R., Bacmeister, J., Takacs, L., Liu, H.-C., Gu, W., Sienkiewicz, M., Koster, R., Gelaro, R., Stajner, I., and Nielsen, J. E.: The GEOS-5 Data Assimilation System – Documentation of Versions 5.0.1 and 5.1.0, NASA Technical Report Series on Global Modeling and Data Assimilation, 27, <https://doi.org/10.5067/Y9NZMZ24W48G>, 2008.
- 640 Seager, R., Naik, N., and Vecchi, G. A.: Thermodynamic and dynamic mechanisms for large-scale changes in the hydrological cycle in response to global warming, *Journal of Climate*, 23, 4651–4668, 2010.
- Song, C., McCoy, D. T., Eidhammer, T., Gettelman, A., McCoy, I. L., Watson-Parris, D., Wall, C. J., Elsaesser, G., and Wood, R.: Buffering of Aerosol-Cloud Adjustments by Coupling Between Radiative Susceptibility and Precipitation Efficiency, *Geophysical Research Letters*, 51, e2024GL108663, <https://doi.org/10.1029/2024GL108663>, publisher: John Wiley & Sons, Ltd, 2024.
- 645 Suarez, M., Schopf, P. S., and Nielsen, J. E.: MAPL: A high-level programming paradigm to support the development of large, multiscale Earth system models, *Bulletin of the American Meteorological Society*, 88, 865–878, <https://doi.org/10.1175/BAMS-88-6-865>, 2007.
- Takacs, L. L., Suárez, M. J., and Todling, R.: The Stability of Incremental Analysis Update, *Monthly Weather Review*, 146, 3259–3275, 2018.
- 650 Tan, I. and Barahona, D.: The impacts of immersion ice nucleation parameterizations on Arctic mixed-phase stratiform cloud properties and the Arctic radiation budget in GEOS-5, *Journal of Climate*, 35, 4049–4070, <https://doi.org/10.1175/JCLI-D-21-0368.1>, 2022.
- Tompkins, A., Cardinali, C., Morcrette, J.-J., and Rodwell, M.: Influence of aerosol climatology on forecasts of the African Easterly Jet, *Geophysical research letters*, 32, 2005.
- Twohy, C. H., Coakley, J. A., and Tahnk, W. R.: Effect of changes in relative humidity on aerosol scattering near clouds, *Journal of Geophysical Research: Atmospheres*, 114, n/a–n/a, <https://doi.org/10.1029/2008JD010991>, 2009.
- 655 Twomey, S.: Influence of pollution on shortwave albedo of clouds, *Journal of the Atmospheric Sciences*, 34, 1149–1152, [https://doi.org/10.1175/1520-0469\(1977\)034<1149:tiopot>2.0.co;2](https://doi.org/10.1175/1520-0469(1977)034<1149:tiopot>2.0.co;2), 1977.
- Ullrich, R., Hoose, C., Möhler, O., Niemand, M., Wagner, R., Höhler, K., Hiranuma, N., Saathoff, H., and Leisner, T.: A new ice nucleation active site parameterization for desert dust and soot, *Journal of the Atmospheric Sciences*, 74, 699–717, <https://doi.org/10.1175/JAS-D-16-0074.1>, 2017.
- 660 Uno, I., Eguchi, K., Yumimoto, K., Takemura, T., Shimizu, A., Uematsu, M., Liu, Z., Wang, Z., Hara, Y., and Sugimoto, N.: Asian dust transported one full circuit around the globe, *Nature Geoscience*, 2, 557–560, 2009.
- Wall, C. J., Norris, J. R., Possner, A., McCoy, D. T., McCoy, I. L., and Lutsko, N. J.: Assessing effective radiative forcing from aerosol–cloud interactions over the global ocean, *Proceedings of the National Academy of Sciences*, 119, e2210481119, <https://doi.org/10.1073/pnas.2210481119>, publisher: Proceedings of the National Academy of Sciences, 2022.
- 665 Wood, R.: Stratocumulus Clouds, *Monthly weather review*, 140, 2373–2423, <https://doi.org/10.1175/MWR-D-11-00121.1>, 2012.
- Wood, R., Leon, D., Lebsock, M., Snider, J., and Clarke, A. D.: Precipitation driving of droplet concentration variability in marine low clouds, *Journal of Geophysical Research: Atmospheres*, 117, n/a–n/a, <https://doi.org/10.1029/2012jd018305>, 2012.
- Yuan, T., Song, H., Oreopoulos, L., Wood, R., Bian, H., Breen, K., Chin, M., Yu, H., Barahona, D., Meyer, K., et al.: Abrupt reduction in shipping emission as an inadvertent geoengineering termination shock produces substantial radiative warming, *Communications Earth & Environment*, 5, 281, 2024.
- 670



- Zhang, J., Reid, J. S., Christensen, M., and Benedetti, A.: An evaluation of the impact of aerosol particles on weather forecasts from a biomass burning aerosol event over the Midwestern United States: observational-based analysis of surface temperature, *Atmospheric Chemistry and Physics*, 16, 6475–6494, <https://doi.org/10.5194/acp-16-6475-2016>, 2016a.
- 675 Zhang, Z., Werner, F., Cho, H.-M., Wind, G., Platnick, S., Ackerman, A., Di Girolamo, L., Marshak, A., and Meyer, K.: A framework based on 2-D Taylor expansion for quantifying the impacts of subpixel reflectance variance and covariance on cloud optical thickness and effective radius retrievals based on the bispectral method, *Journal of Geophysical Research: Atmospheres*, 121, 7007–7025, 2016b.

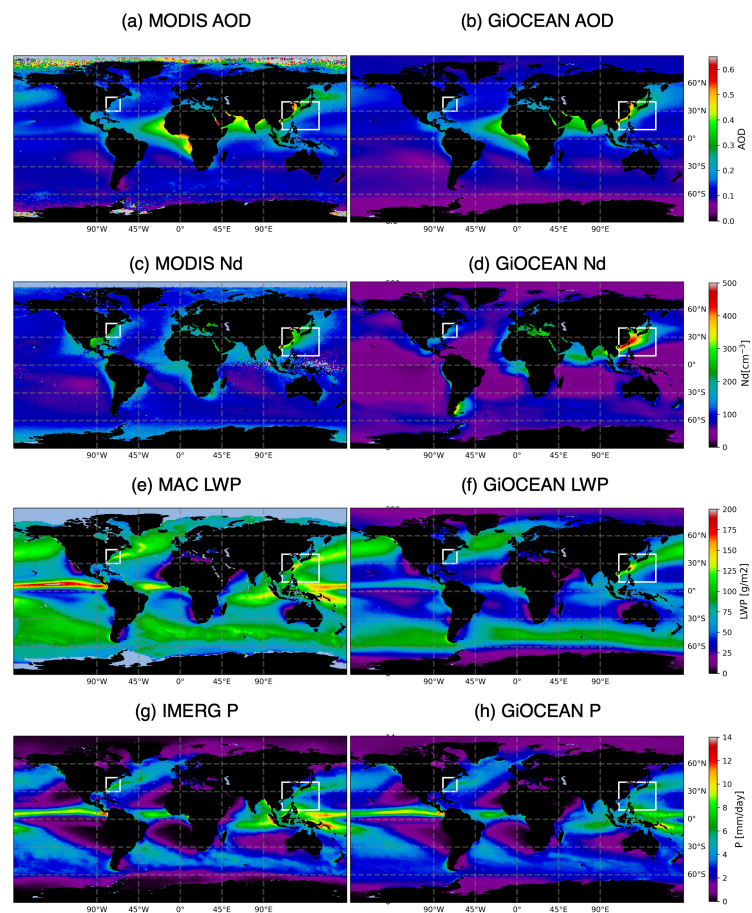


Figure 1. Comparison of the variables examined in this study between remote sensing observations (a,c,e,g) and GiOcean (b,d,f,h). GiOcean aerosol optical depth is compared to MODIS (a,b); Nd is compared to MODIS (c,d); liquid water path is compared to MAC (e,f); and precipitation is compared to IMERG (g,h). Study areas off the coast of the US and China are highlighted in white.

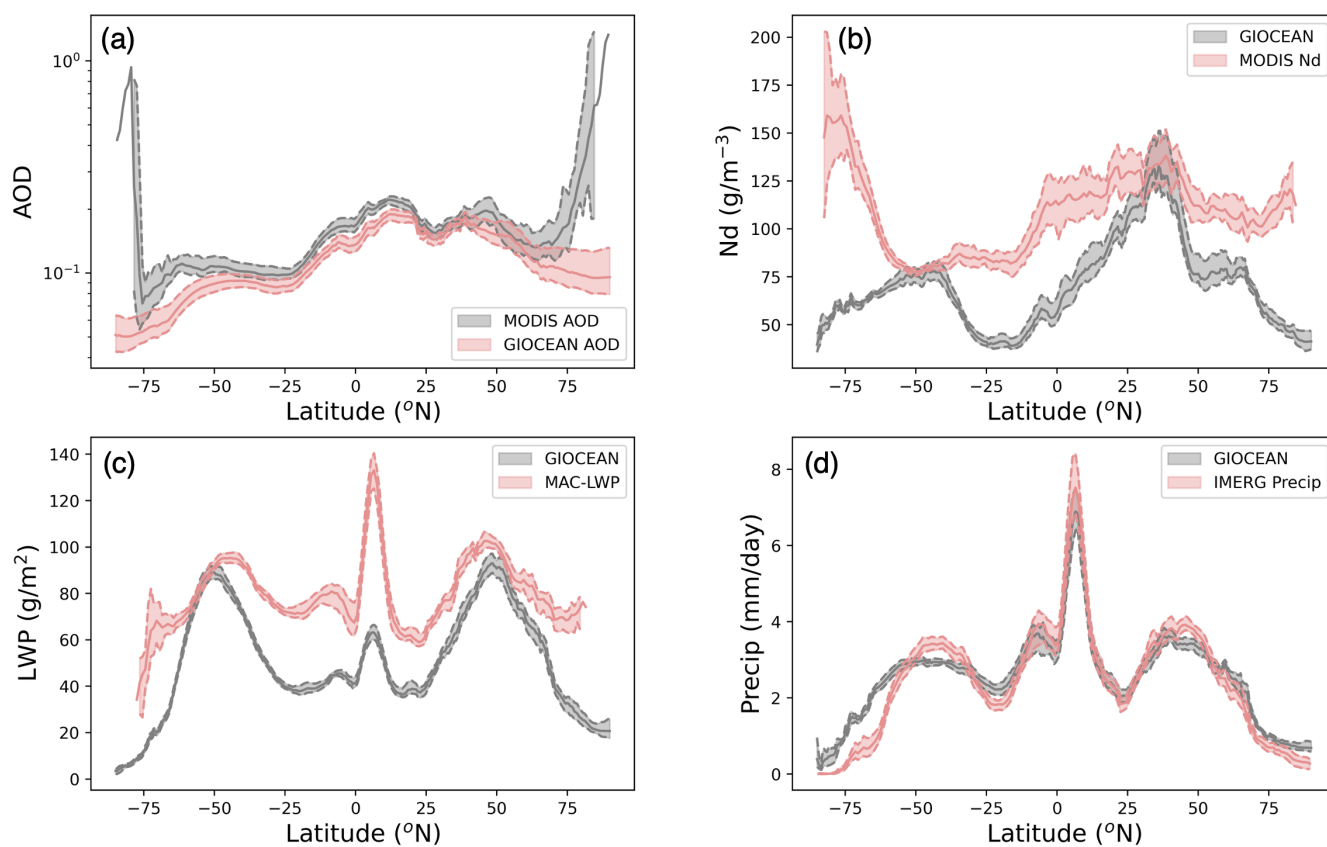


Figure 2. Comparison of zonal-mean oceanic quantities from GiOcean (a) aerosol optical depth from MODIS; (b) precipitation rate from IMERG; (c) LWP from MAC-LWP; (d) Nd from MODIS. Shading denotes inter-annual variability.

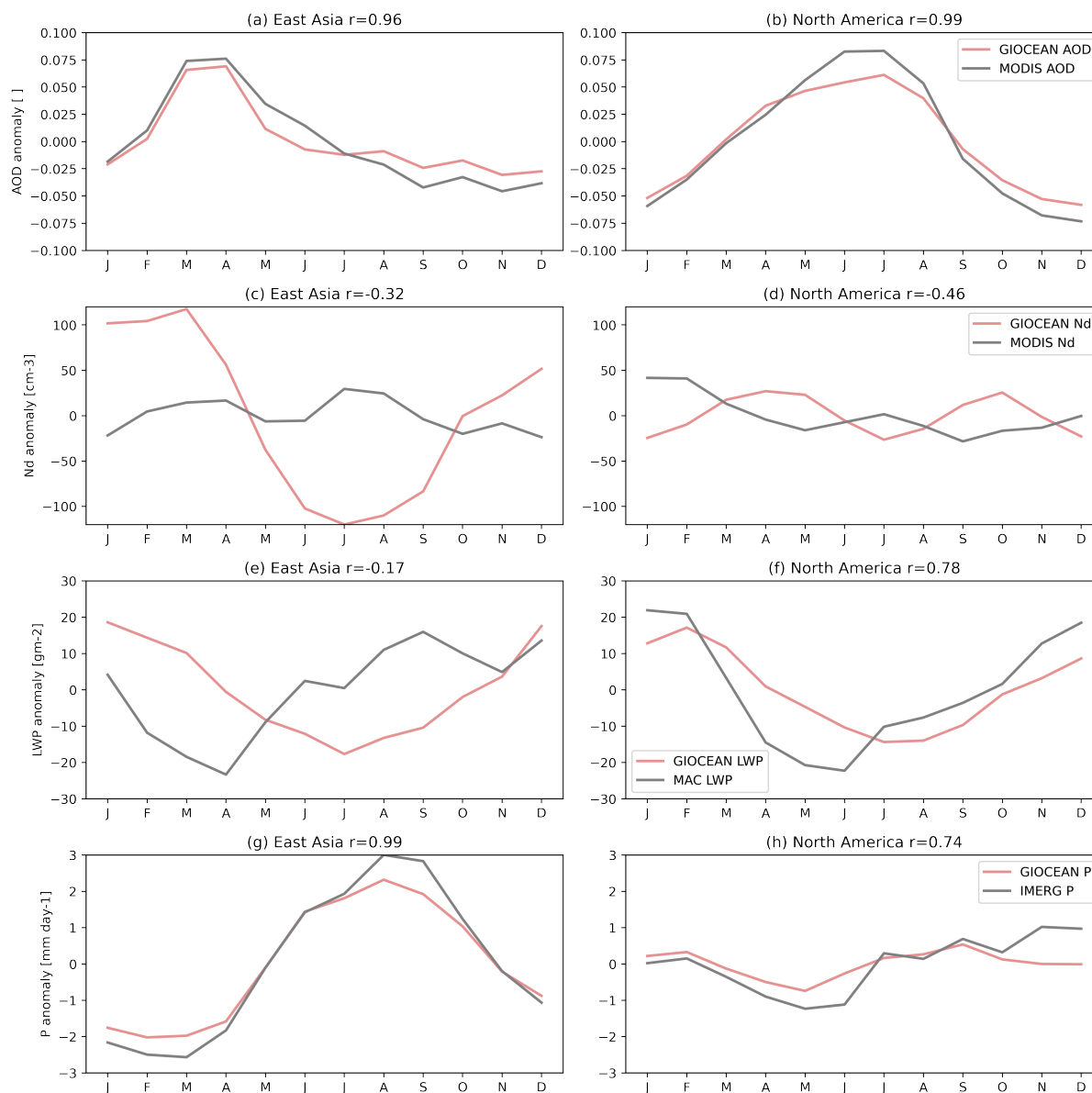


Figure 3. Comparison of seasonal cycles in the outflow regions of East Asia (a,c,e,g) and North America (b,d,f,h) for AOD (ab), Nd (cd), LWP (ef), and precipitation rate (gh).

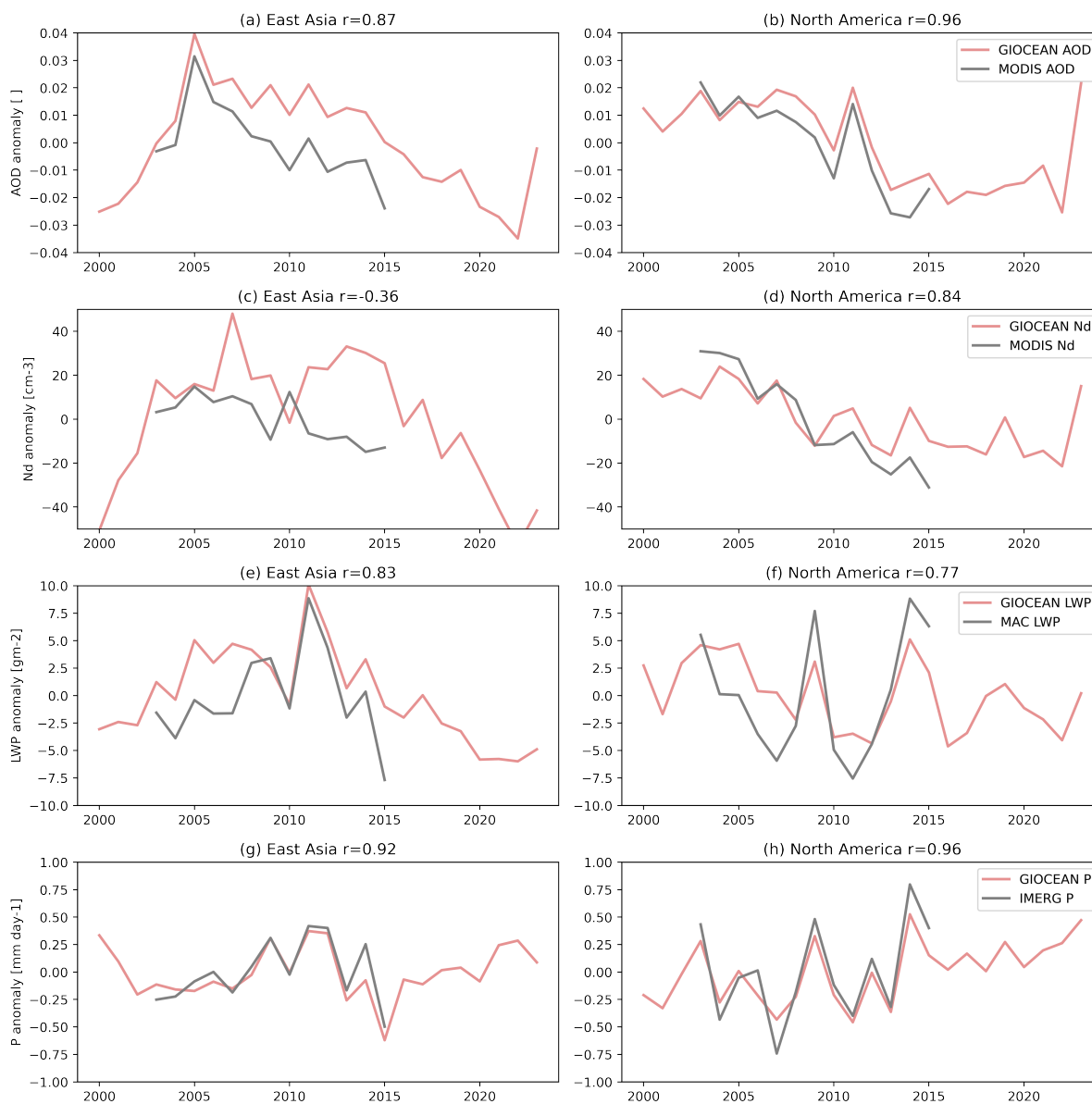


Figure 4. Comparison of decadal trends in the outflow regions of East Asia (a,c,e,g) and North America (b,d,f,h) for AOD (ab), Nd (cd), LWP (ef), and precipitation rate (gh).

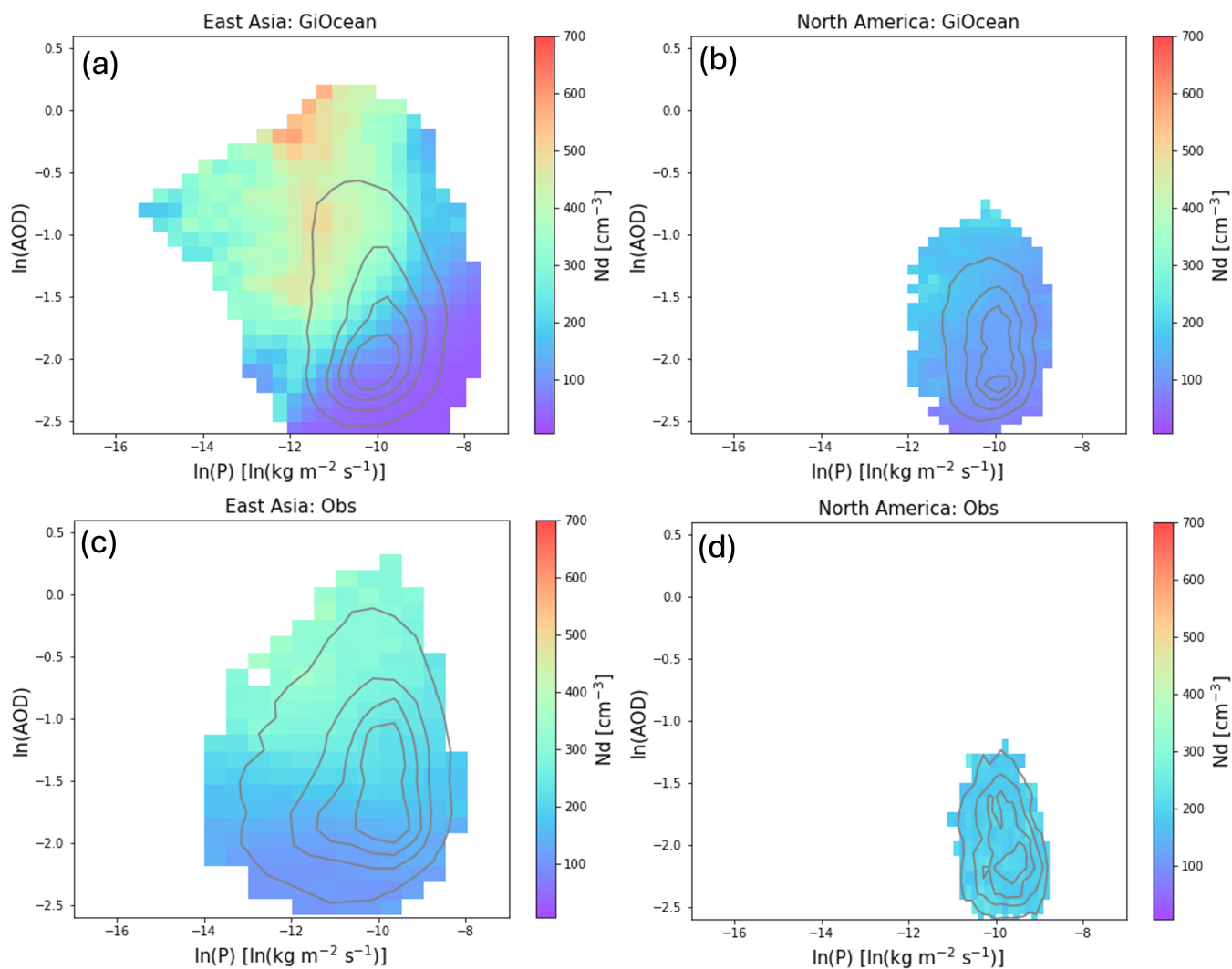


Figure 5. Cloud droplet number composited on AOD and precipitation rate in GiOcean (ab) and from observations (cd) and in the regions off the coast of East Asia (ac) and North America (bd). The density of points in each bin is indicated with grey contours. NB redo plots with 30+min points.

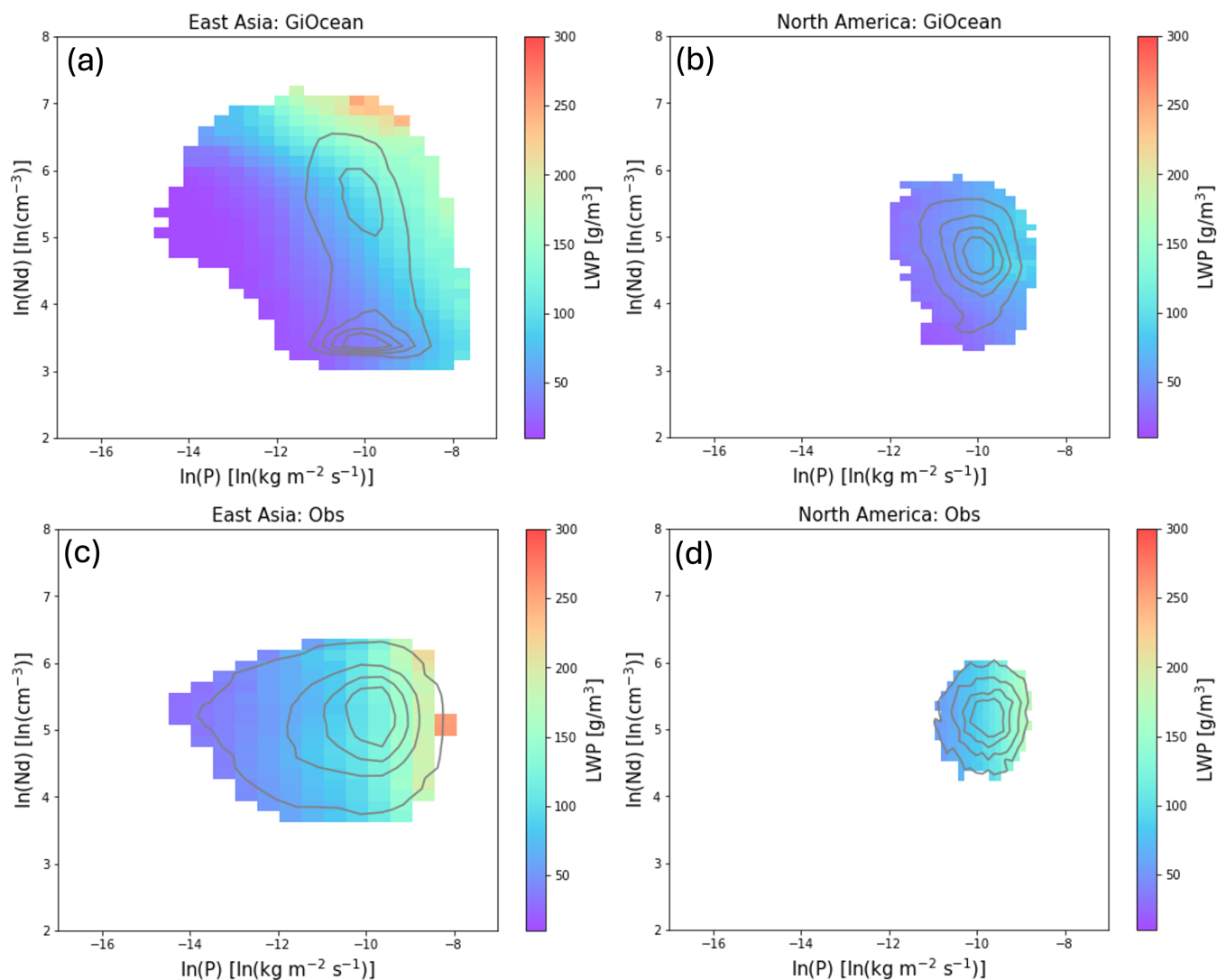


Figure 6. Liquid water path composited on Nd and precipitation rate in GiOcean (ab) and from observations (cd) and in the regions off the coast of East Asia (ac) and North America (bd). The density of points in each bin is indicated with grey contours. NB redo plots with 30+-min points.

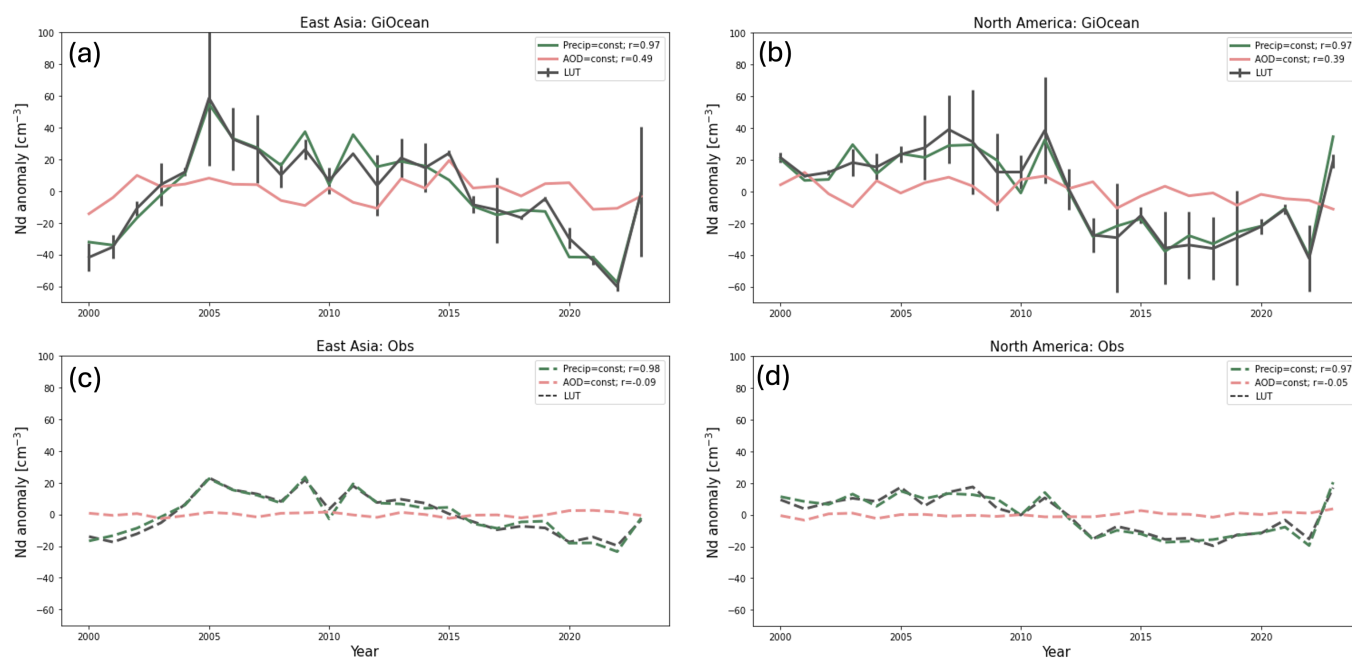


Figure 7. The decadal trend in Nd in GiOcean (ab) and from observations (cd) and in the regions off the coast of East Asia (ac) and North America (bd) as predicted by the look up table in Figure 5. The residual between the look up table prediction and model is shown using error bars. Setting AOD or precipitation equal to a constant value is shown in pink and green, respectively. Using the look up table from GiOcean (Figure 5ab) is shown using solid lines. Using the look up table from observations (Figure 5cd) is shown using dashed lines. Correlation coefficient (r) is calculated between the decadal trend of Nd with look up table predictions with fixed sink and source, respectively.

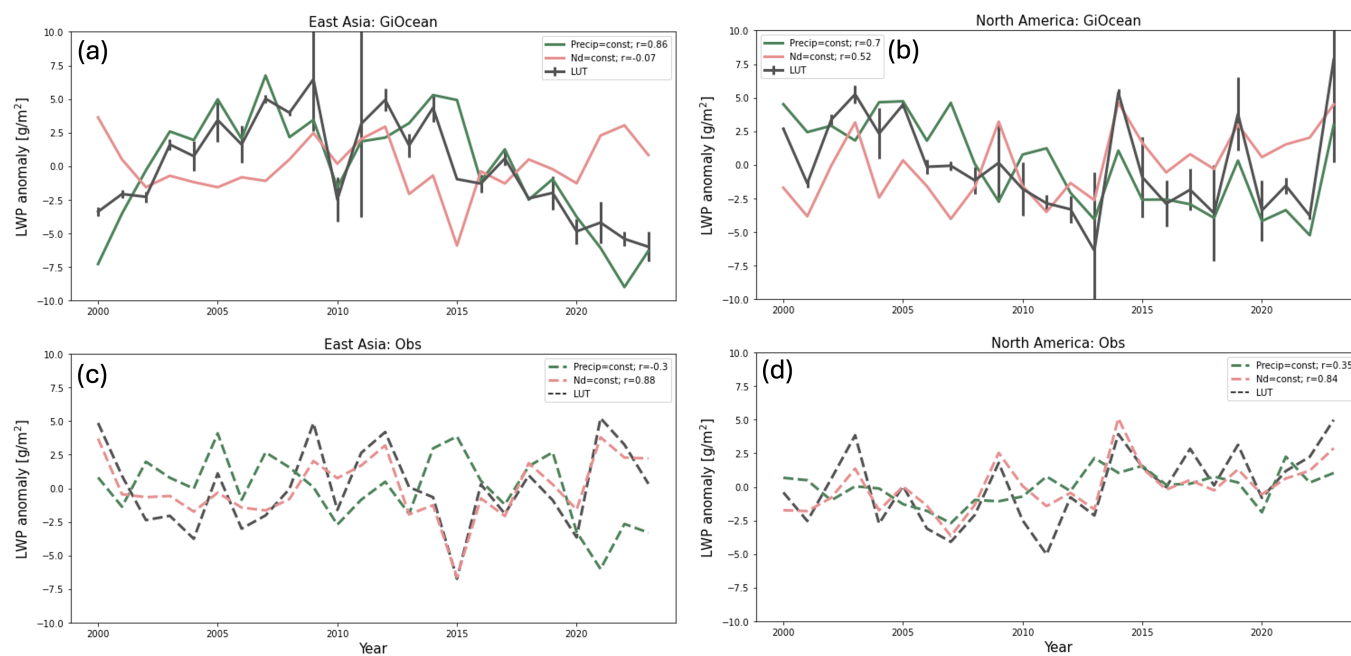


Figure 8. The decadal trend in LWP in GiOcean (ab) and from observations (cd) and in the regions off the coast of East Asia (ac) and North America (bd) as predicted by the look up table in Figure 5. The residual between the look up table prediction and model is shown using error bars. Setting Nd or precipitation equal to a constant value is shown in pink and green, respectively. Using the look up table from GiOcean (Figure 5ab) is shown using solid lines. Using the look up table from observations (Figure 5cd) is shown using dashed lines. Correlation coefficient (r) is calculated between the decadal trend of LWP with look up table predictions with fixed sink and source, respectively.